

STUDY OF ^{60}Zn AND ^{61}Zn

D.J. WEBER, G.M. CRAWLEY, W. BENENSON, E. KASHY, and H. NANN
Cyclotron Laboratory and Physics Department
Michigan State University, East Lansing, MI 48824

Abstract: The ($^{12}\text{C}, ^{10}\text{Be}$) and ($^{12}\text{C}, ^9\text{Be}$) reactions on ^{58}Ni were studied at 77 MeV. New levels were determined for both residual nuclei, ^{60}Zn and ^{61}Zn . In the case of ^{61}Zn a significant difference from the previously accepted mass was verified by means of the $^{64}\text{Zn}(^3\text{He}, ^6\text{He})$ reaction, and levels in ^{61}Zn were also observed in this reaction. The new mass excess for ^{61}Zn is 56205 ± 20 keV. Angular distributions for the ^{12}C induced reactions are compared with finite range DWBA calculations and found to be insensitive to L- and J-transfer.

NUCLEAR REACTIONS $^{58}\text{Ni}(^{12}\text{C}, ^{10}\text{Be})$, $^{58}\text{Ni}(^{12}\text{C}, ^9\text{Be})$, $E=77$ MeV; measured ($E_{^{10}\text{Be}}$, θ), ($E_{^9\text{Be}}$, θ). ^{60}Zn , ^{61}Zn deduced levels. $^{64}\text{Zn}(^3\text{He}, ^6\text{He})$, $E=70$ MeV; ^{61}Zn deduced levels. Enriched targets. ATOMIC MASS ^{61}Zn .

1. Introduction

Very little is known about the most proton rich zinc isotopes ^{60}Zn and ^{61}Zn . They were included, however, in the recent shell model calculations of the zinc isotopes by van Hienen, Chung, and Wildenthal,¹⁾ which included $2p_{3/2}$, $1f_{5/2}$, and $2p_{1/2}$ orbitals outside an inert ^{56}Ni core. The nucleus ^{60}Zn has only been studied by the $^{58}\text{Ni}(^3\text{He}, n)$ reaction with an energy resolution between 300 and 500 keV FWHM²⁻⁴⁾ and by a ($^3\text{He}, n$) experiment⁵⁾ which measured the energies of four excited states up to 4.2 MeV of excitation with high precision. In the case of ^{61}Zn , no level scheme exists, and the mass excess measurements via beta-decay⁶⁾ and the $^{58}\text{Ni}(^4\text{He}, n)$ threshold⁷⁾ are imprecise and in poor agreement with each other.

With the availability of heavy ion beams, ^{60}Zn and ^{61}Zn are now accessible to study by charged particle reactions, and good energy resolution (≈ 150 keV FWHM) can be obtained over a wide range of excitation energies. Heavy ion transfer reactions tend, however, to favor final states of higher spin than do the ($^3\text{He}, n$) and ($^4\text{He}, n$) reactions and therefore would tend to complement rather than reproduce the results of these experiments. For the case of $^{58}\text{Ni}(^{12}\text{C}, ^{10}\text{Be})$ at 77 MeV, a simple semiclassical picture⁸⁾ shows that the favored L-transfer is about 5. The favored Q-value for $L=0$ is at $E_x \approx -4$ MeV whereas for $L=5$ it is at $E_x \approx 2$ MeV. Thus, low spin states which are observed preferentially in ($^3\text{He}, n$) at forward angles, should be weak in this experiment. Besides the new information one can gain on

states agreed with the accepted energies⁹) of these levels within 30 keV, the accuracy of the energy determination.

Since the ground state of ^{61}Zn was found to be 350 ± 50 keV from the accepted value,¹⁰) this result was checked with the $^{64}\text{Zn}(^3\text{He}, ^6\text{He})$ reaction at 70 MeV. The detection apparatus was identical to that described above except that a 50 cm long detector was used enabling a single spectrum to measure up to 10 MeV of excitation. Particle identification was again unambiguous.

The ^{64}Zn target was a self-supporting foil $490 \pm 35 \mu\text{g}/\text{cm}^2$ thick enriched to 99.32% of ^{64}Zn . The spectra were calibrated using the reaction $^{56}\text{Fe}(^3\text{He}, ^6\text{He})$ to known states of ^{53}Fe . The ^{56}Fe target was a self-supporting foil $976 \pm 35 \mu\text{g}/\text{cm}^2$ thick. The calibration was corrected for the differential energy loss of ^3He and ^6He ions in the two targets. The cross section for the strongest state at $\theta_L = 9^\circ$ was only 120 ± 20 nb/sr. As a result of the weak cross sections for states in ^{61}Zn excited in the reaction $^{64}\text{Zn}(^3\text{He}, ^6\text{He})$, data were taken at only two angles, $\theta_L = 9^\circ$ and 7° . Several spectra were taken at 9° however, with calibration runs at the same angle preceding and following each run to check for beam energy drifts.

3. Results

3a. ^{60}Zn

A ^{10}Be energy spectrum at $\theta_{\text{lab}} = 10^\circ$ is shown in fig. 1. The energy levels observed are listed in Table 1, together with the previously observed levels. They are also displayed in fig. 2, together with the known levels and the predictions of

the levels of ^{60}Zn and ^{61}Zn , the reaction mechanism itself is of interest since the $(^{12}\text{C}, ^{10}\text{Be})$ and $(^{12}\text{C}, ^9\text{Be})$ reactions have not been extensively studied for targets above $A = 40$.

2. Experiment

For the heavy ion induced reactions, a beam of 77 MeV $^{12}\text{C}^{4+}$ ions was obtained in the Michigan State University cyclotron. The reactions products were detected on the focal plane of an Engle split-pole spectrograph. The detector was 14.5 cm long and consisted of two resistive wire proportional counters backed by a thin plastic scintillator. Position along the focal plane, energy loss in the front proportional counter, light output in the scintillator, and time of flight relative to the cyclotron r.f. were all stored in the computer for off-line sorting. An additional gate was set on the energy loss in the back proportional counter to reduce the recording on tape of unwanted particles. Particle identification proved unambiguous. The spectra were taken in two steps, one for the low excitation region and one for the high excitation region. The spectra were calibrated by varying the spectrometer field to move elastically scattered $^{12}\text{C}^{5+}$ particles across the detector. These particles had approximately the same rigidity as the ^9Be and ^{10}Be particles of interest. The target was a self-supporting foil $324 \pm 20 \mu\text{g}/\text{cm}^2$ thick enriched to 99.89% of ^{58}Ni . The calibration was corrected for the differential energy loss of the ^{12}C , ^{10}Be , and ^9Be ions in the target. This correction was checked by a determination of the energies of the first two excited states of ^{60}Zn populated by the reaction $^{58}\text{Ni}(^{12}\text{C}, ^{10}\text{Be})$. The corrected energies of those

van Hienen et al.¹⁾ below 5 MeV. The ground state is very weakly excited, having a maximum cross section of only 1 $\mu\text{b}/\text{sr}$. Several new states are observed. Two of these, at 4.36 and 5.35 MeV of excitation, dominate the spectra at all angles. The state at 3.62 MeV is a doublet; probably an admixture of the known 3^- state at 3.50 MeV and a new state near 3.70 MeV. Except for weak states at 6.26 and 8.85 MeV, no individual levels are resolvable from the substantial strength observed above 6 MeV of excitation.

Angular distributions for the states in ^{60}Zn are shown in figs. 3 and 4. As in previous ($^{12}\text{C}, ^{10}\text{Be}$) and ($^{16}\text{O}, ^{14}\text{C}$) two proton transfer experiments on lighter nuclei^{11,12)} performed well above the Coulomb barrier, little or no structure is observed in any of these angular distributions, each of which exhibits an exponential decrease with increasing scattering angle. For the excited states, this occurs as a result of the interference between contributions from the different magnetic substates.¹²⁾ Since all of the angular distributions are similar in shape, no spin assignments can be made on the basis of their shapes. However, the momentum conditions do suggest that the strongest states observed have high spin. The only high spin state predicted by van Hienen et al.¹⁾ is a 6^+ state at 4.23 MeV, which may correspond to the observed 4.36 MeV state. It is very likely, however, that high spin states would contain $1g_{9/2}$ admixtures not included in the shell model calculations.¹³⁾

3b. ^{61}Zn

The mass excess of ^{61}Zn as measured by $^{58}\text{Ni}(^{12}\text{C}, ^9\text{Be})$ and $^{64}\text{Zn}(^3\text{He}, ^6\text{He})$ reactions were lower than the previously accepted value¹⁰⁾ by 350 ± 50 and 375 ± 20 keV, respectively. Using the latter, we obtain a new mass excess of -56205 ± 20 keV in disagreement with both of the previous mass measurements. The accepted mass of ^{61}Zn is based on the end point of the β -spectrum. This study may have had difficulties with non-linearities in the Kurie plots near the end points, and therefore the 200 keV error quoted is certainly too small. The $^{58}\text{Ni}(\alpha, n)$ threshold energy determination found a mass excess 510 keV higher than the β -decay result with an error of 30 keV. Mass measurements of ^{66}Ga and ^{63}Zn from that study also disagree with the presently accepted values. It is probable that the assumption of s-wave neutron production by the (α, n) reaction on ^{58}Ni at threshold is partly responsible for this disagreement.

Spectra from both the reactions used to study ^{61}Zn are given in fig. 5. The energy levels observed are given in Table II and fig. 6 for the heavy and light ion experiments separately. The predictions of van Hienen et al. are also given. Since the calculation predicts a very high level density above 1.5 MeV, only the states below this excitation energy are shown. The states at $1.25 \pm .02$, $2.32 \pm .02$, and $2.66 \pm .02$ MeV excited in the lighter ions reactions have corresponding levels at $1.19 \pm .05$, $2.29 \pm .05$, and $2.59 \pm .05$ MeV in the heavy ion spectrum. Two low-lying levels at $0.88 \pm .02$ and $2.08 \pm .02$ MeV excited in the ($^3\text{He}, ^6\text{He}$) reaction do not, however, appear to

have corresponding levels in the $(^{12}\text{C}, ^9\text{Be})$ reaction. A very weak state in the $(^3\text{He}, ^6\text{He})$ spectrum near 3.2 MeV may correspond to the 3.22 MeV level in the $(^{12}\text{C}, ^{10}\text{Be})$ spectrum. Above the 3.5 MeV, however, there is little or no correspondence between the levels excited by the two reactions. This is not surprising in view of the different configurations favored by the pickup and stripping reactions and in view of the momentum matching conditions for the $(^{12}\text{C}, ^9\text{Be})$ reaction which favor the excitation of high spin states. A high level density in the lighter ion spectrum makes it impossible to discern individual states above 5.5 MeV excitation.

Angular distributions for the states in $^{58}\text{Ni}(^{12}\text{C}, ^9\text{Be})$ are shown in figs. 7 and 8. Like the $^{58}\text{Ni}(^{12}\text{C}, ^{10}\text{Be})$ results, they are all relatively structureless and lack j -dependence, and the cross sections for all states decrease exponentially with increasing scattering angle. There appears, however, to be some forward angle structure for the highly excited states at 5.13 and 5.59 MeV.

4. Calculations

The DWBA calculations which were carried out for the heavy ion reactions were performed with the code LOLA.¹⁴ Cluster transfer of the two or three particles was assumed, and a radius of $1.15 (A^{1/3} + 2^{1/3})$ and a diffuseness of 0.65 fm were used to calculate the bound state wave functions with the depth adjusted to fit the separation energy. The optical model parameters were taken from a study of $^{26}\text{Mg}(^{12}\text{C}, ^{10}\text{Be})$ at 46 MeV,¹² and are given

in Table III. A slight enlargement of the real diffuseness in the exit channel over the Ref. 12 values was found to improve the fit in all cases. No attempt was made to compare the absolute value of the cross sections to the calculations since the spins and structures of most of the states are unknown. The curves shown were therefore individually normalised to the data.

The results for the $L = 0, 2, 3$, and 4 calculations for the $^{58}\text{Ni}(^{12}\text{C}, ^{10}\text{Be})$ reaction are compared to the data in Fig. 4. Although the very weak ground state has poor statistics, it appears to support the strong oscillations given by the LOLA calculations. For the excited states the data and the calculation exhibit little angular structure or L -transfer dependence.

The calculations for $^{58}\text{Ni}(^{12}\text{C}, ^9\text{Be})$ are compared to the data in fig. 7. As the spin of the ground state is known to be $3/2^-$ from the log ft of the β -decay, the ground state has been compared to the calculation for a j transfer of $3/2$. Calculations for j transfers of $1/2$ and $5/2$ are shown with the first excited state angular distribution. None of the experimental angular distributions, including that of the known $3/2^-$ ground state,¹⁵ shows the rapid oscillations predicted for $j = 1/2$ and $3/2$. This indicates a failure in the calculation which is probably associated with the cluster transfer assumption. In this reaction just as in the $^{58}\text{Ni}(^{12}\text{C}, ^{10}\text{Be})$ the lack of structure in the angular distributions precludes any spin assignments.

5. Conclusions

The $^{58}\text{Ni}(^{12}\text{C},^{10}\text{Be})$, $^{58}\text{Ni}(^{12}\text{C},^9\text{Be})$, and $^{64}\text{Zn}(^3\text{He},^6\text{He})$ reactions have been used to study the nuclei ^{60}Zn and ^{61}Zn . A new ground state mass for ^{61}Zn and several new levels for both nuclei were found, but no spin assignments could be made because of the lack of distinguishing features in the angular distributions. Several features of the heavy ion reactions are fairly well reproduced by DWBA calculations, particularly for the $^{58}\text{Ni}(^{12}\text{C},^{10}\text{Be})$ reaction.

Table I.--Energy levels observed in ^{60}Zn .

$^{3}\text{He}, n)^a$	E_x (MeV)		J^π ^d
	$(^3\text{He}, n)^b$	$(^3\text{He}, n\gamma)^c$ present	
0.0	0.0	0.0	0 ⁺
1.019±.010	1.00±.03	1.0042	2 ⁺
2.21±.03	2.20±.03	2.1936	4 ⁺
3.51±.02	3.52±.03	3.5043	3 ⁻
	3.98±.03		1 ⁻
4.18±.03		4.2004	(2 ⁺)
4.93±.04	4.88±.03		2 ⁺
	5.20±.06		2 ⁺
5.49±.03	5.52±.03		2 ⁺ , 4 ⁺
		5.35±.05	
		6.26±.07	0 ⁺
	6.63±.03		0 ⁺
	7.38±.03		(2 ⁺ , 3 ⁻)
	8.73±.03		
		8.85±.08	

- a) Ref. 2)
- b) Ref. 3)
- c) Ref. 5)
- d) Ref. 9)

Table II.--Energy levels observed in ^{61}Zn .

$^{64}\text{Zn} (^3\text{He}, ^6\text{He})$	E_x (MeV)	$^{58}\text{Ni} (^{12}\text{C}, ^9\text{Be})$	$J\pi^a$
	0.0	0.0	$3/2^-$
	$0.88 \pm .02$		
	$1.25 \pm .02$	$1.19 \pm .05$	
	$2.08 \pm .02$		
	$2.32 \pm .02$	$2.29 \pm .05$	
	$2.66 \pm .02$	$2.59 \pm .05$	
		$3.22 \pm .05$	
		$4.20 \pm .05$	
	$4.55 \pm .02$		
	$4.97 \pm .02$		
	$5.15 \pm .02$	$5.13 \pm .05$	
	$5.43 \pm .02$		
		$5.59 \pm .05$	
		$6.29 \pm .05$	
		$6.98 \pm .05$	
		$7.63 \pm .05$	

a) Ref. 15.

Table III.--Optical model parameters used in LOLA¹⁴ calculations.

	$^{12}\text{C} + ^{58}\text{Ni}$	$^{10}\text{Be} + ^{60}\text{Zn}$
V_R (MeV)	100	100
R_R (fm.)	1.24	1.24
a_R (fm.)	0.48	0.75
W_I (MeV)	27	27
R_I (fm.)	1.36	1.36
a_I (fm.)	0.22	0.22

Figure Captions

FIG. 8. Angular distributions for excited states seen in $^{58}\text{Ni}(^{12}\text{C}, ^9\text{Be})^{61}\text{Zn}$.

Fig. 1. An energy spectrum for ^{60}Zn at 77 MeV.

Fig. 2. Energy levels of ^{60}Zn . The levels observed in this experiment are shown in the center. They are compared with the previous⁹ level energies and spins which are shown to the left and the calculated energies and spins of van Hienen et al.¹ which appear to the right.

Fig. 3. Angular distributions for low lying states seen in $^{58}\text{Ni}(^{12}\text{C}, ^{10}\text{Be})^{60}\text{Zn}$. Spins where included are taken from Ref. 9. Fits were made with LOLA¹⁴ and are arbitrarily normalized.

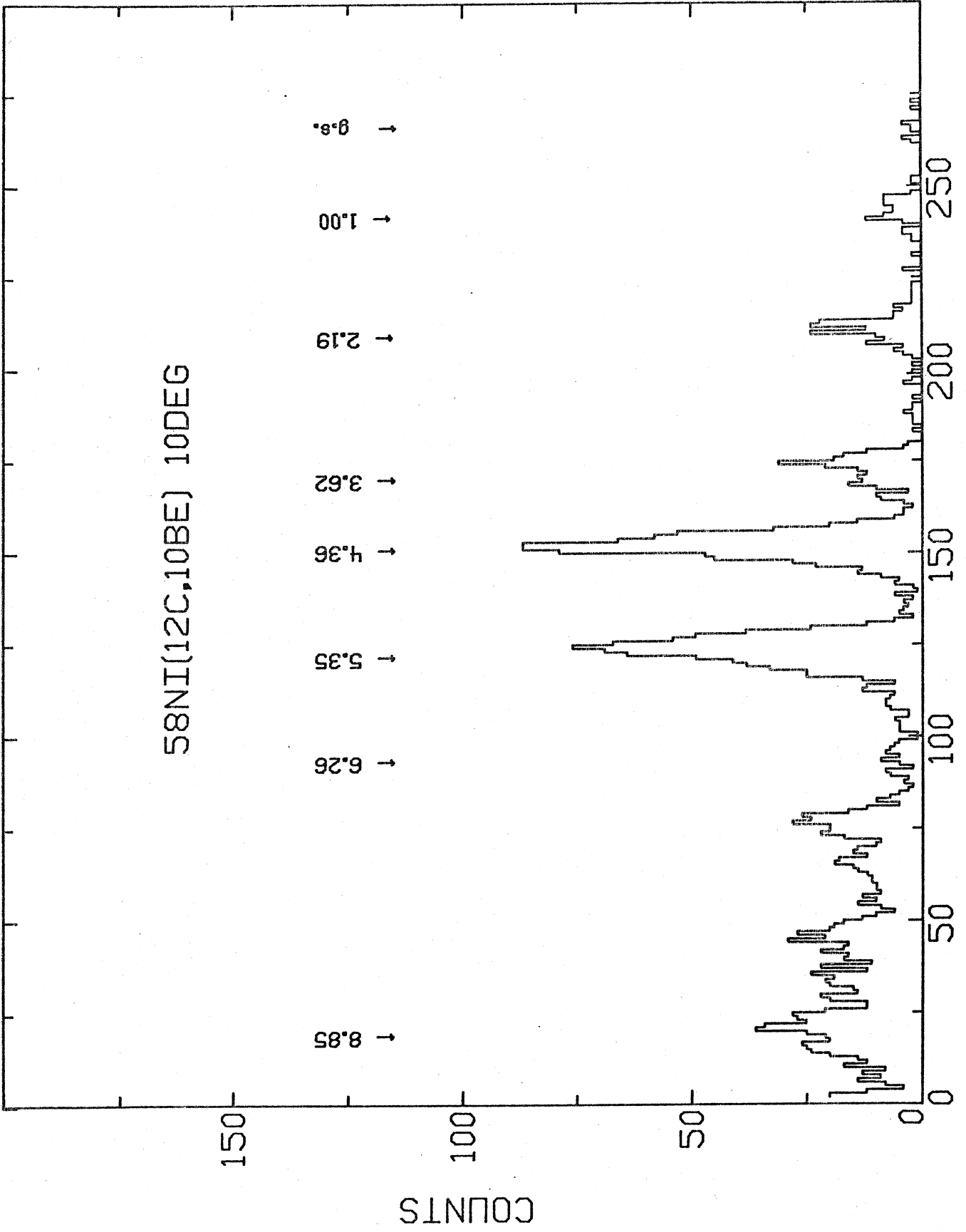
Fig. 4. Angular distributions for excited states seen in $^{58}\text{Ni}(^{12}\text{C}, ^{10}\text{Be})^{60}\text{Zn}$.

Fig. 5. Energy spectra for ^{61}Zn are shown for the reactions $^{64}\text{Zn}(^3\text{He}, ^6\text{He})$ at 70 MeV (top) and $^{58}\text{Ni}(^{12}\text{C}, ^9\text{Be})$ at 77 MeV (bottom). The horizontal scale has been adjusted so that the two energy axes line up.

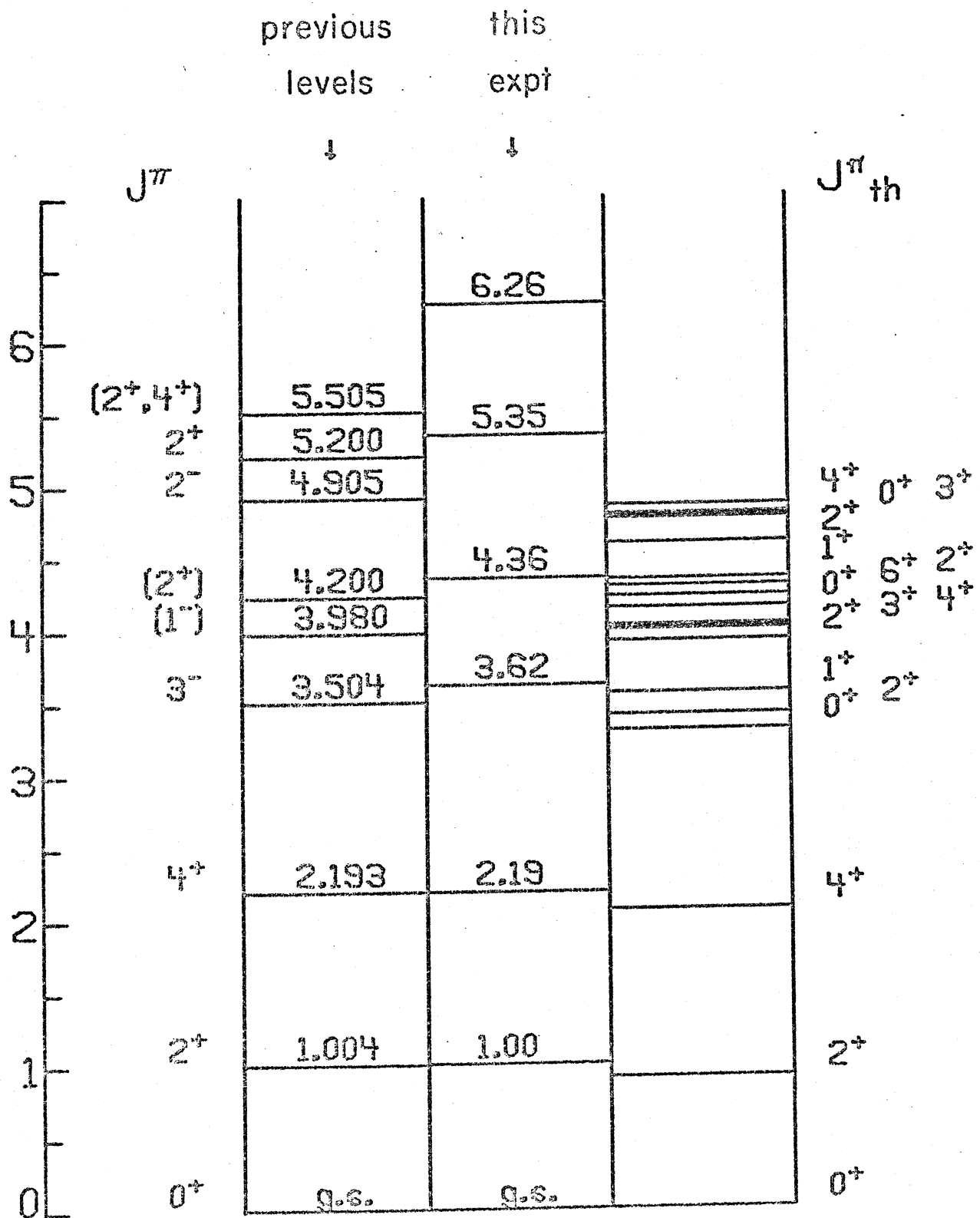
Fig. 6. The energy levels of ^{61}Zn observed in this experiment. The levels on the left are those observed in the reaction $^{58}\text{Ni}(^{12}\text{C}, ^9\text{Be})$; those in the center were seen in the reaction $^{64}\text{Zn}(^3\text{He}, ^6\text{He})$. Theoretical predictions are shown on the right.

Fig. 7. Angular distributions are shown for levels excited in the reaction $^{58}\text{Ni}(^{12}\text{C}, ^9\text{Be})$. Arbitrarily normalized finite range DWBA calculations for various j transfers are shown together with the data.

58NI(12C,10BE) 10DEG



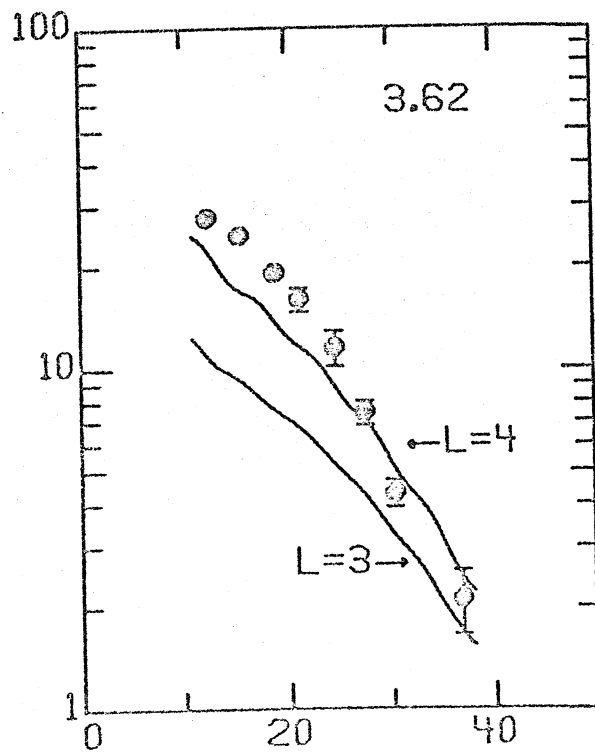
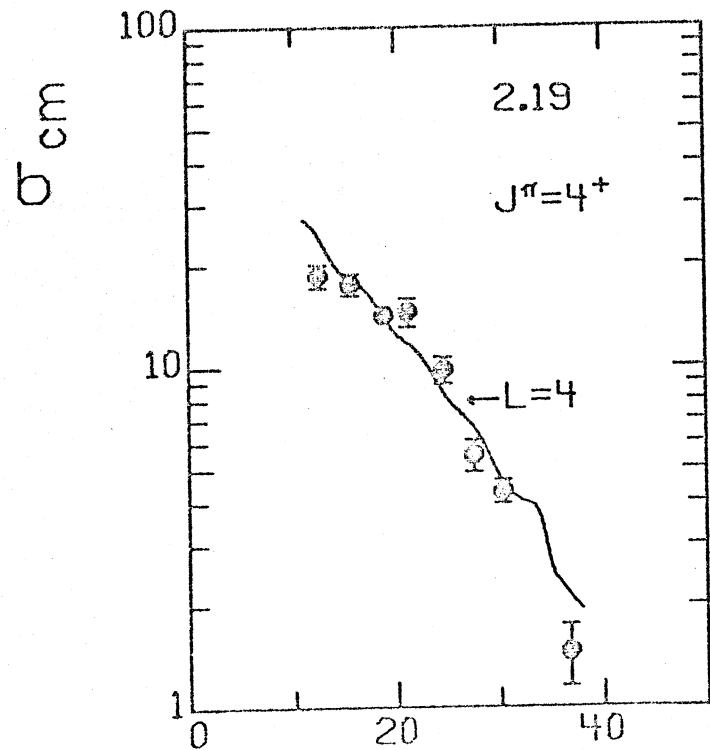
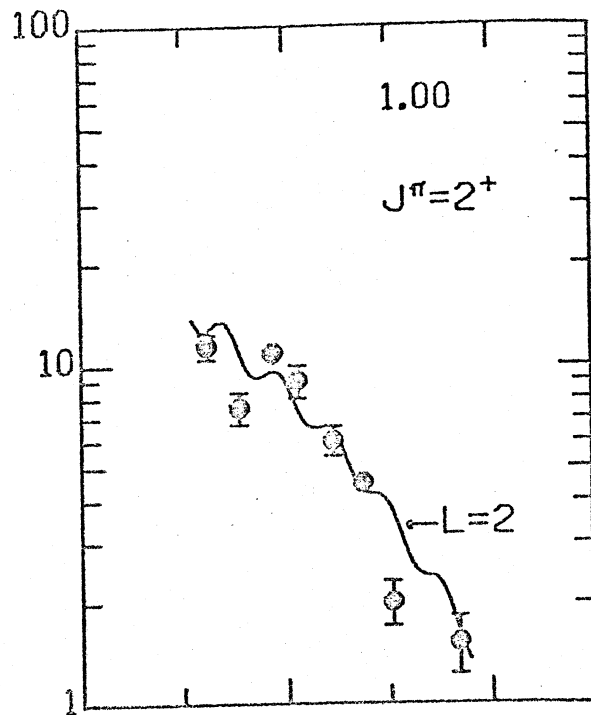
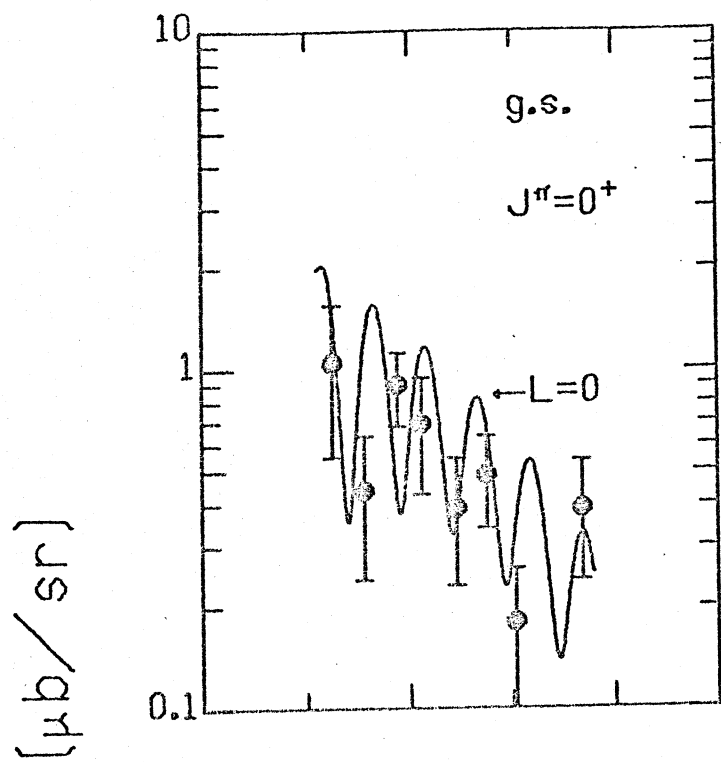
ENERGY (MEV)



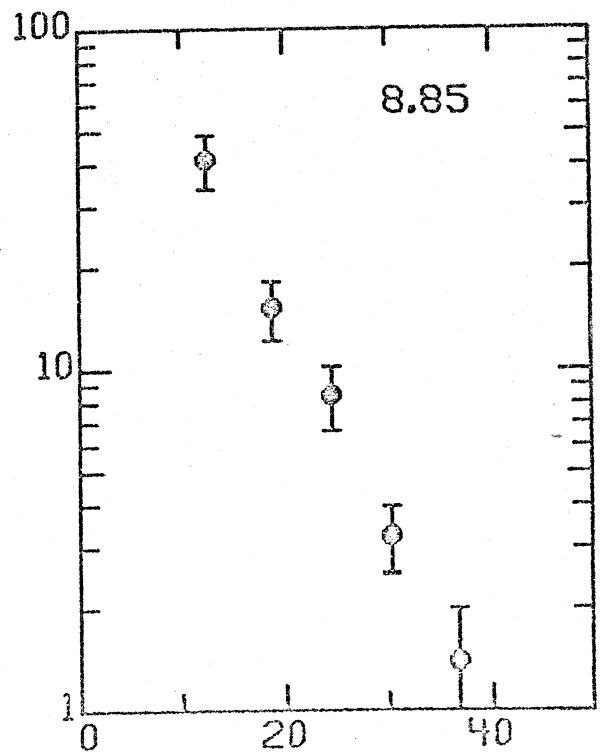
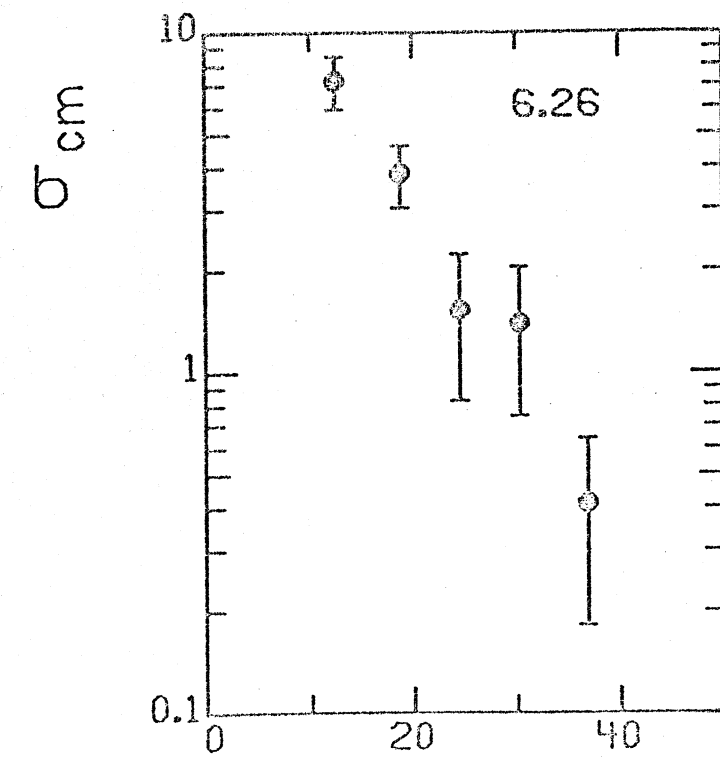
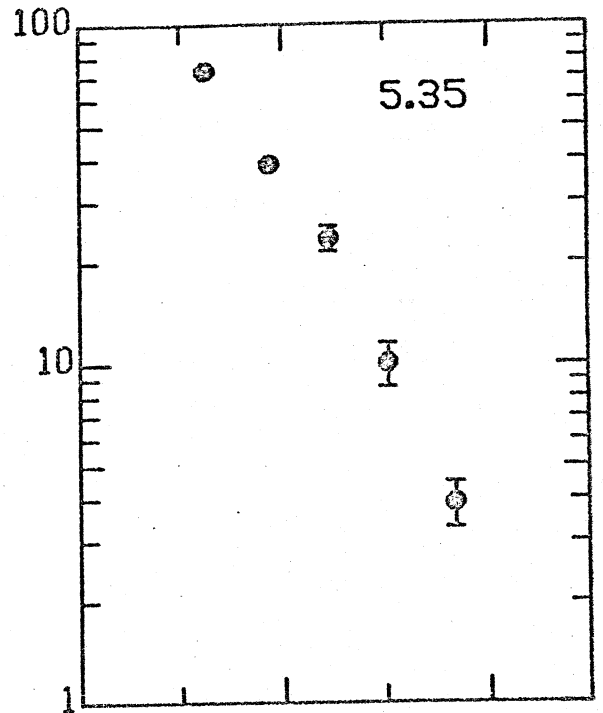
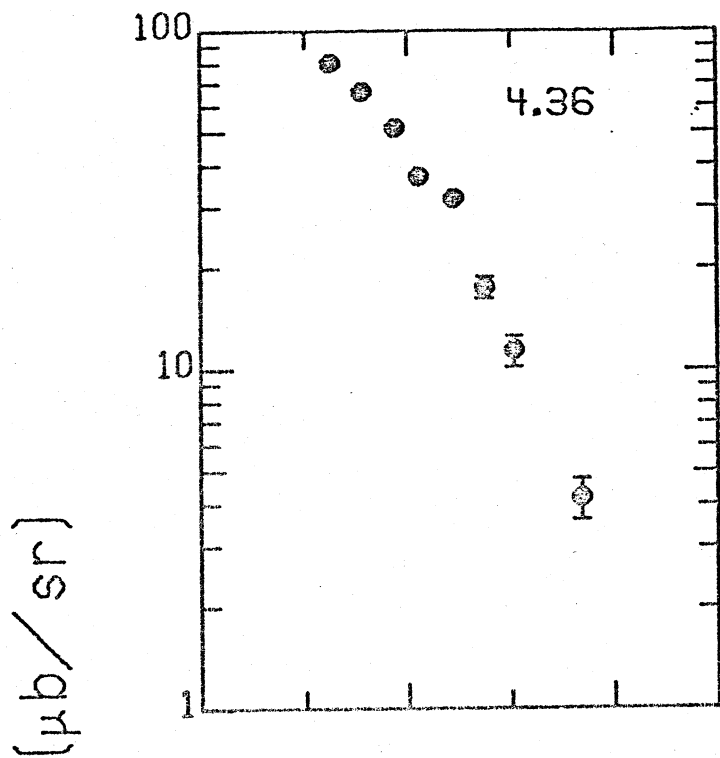
exp.

th.

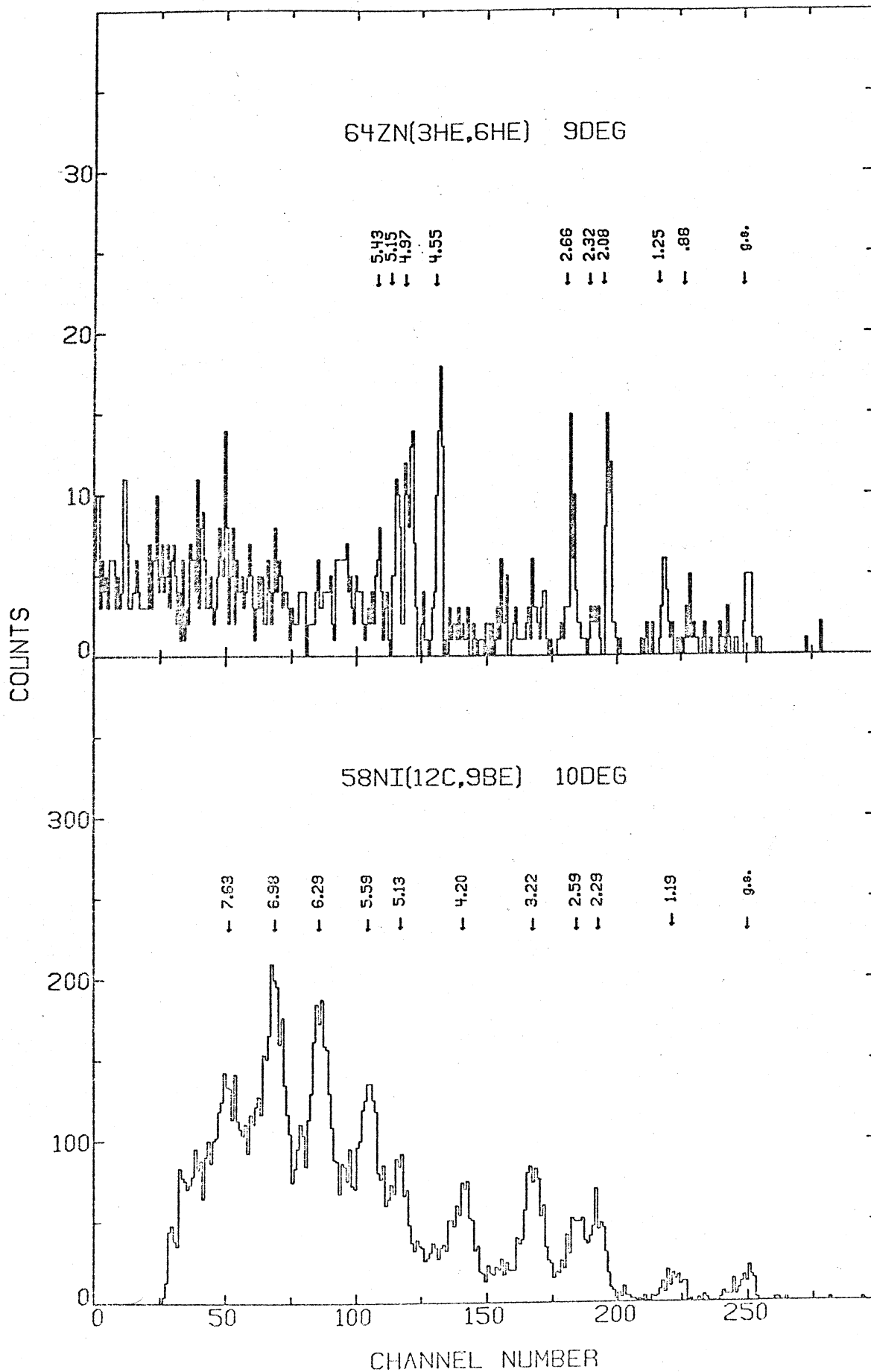
^{60}Zn



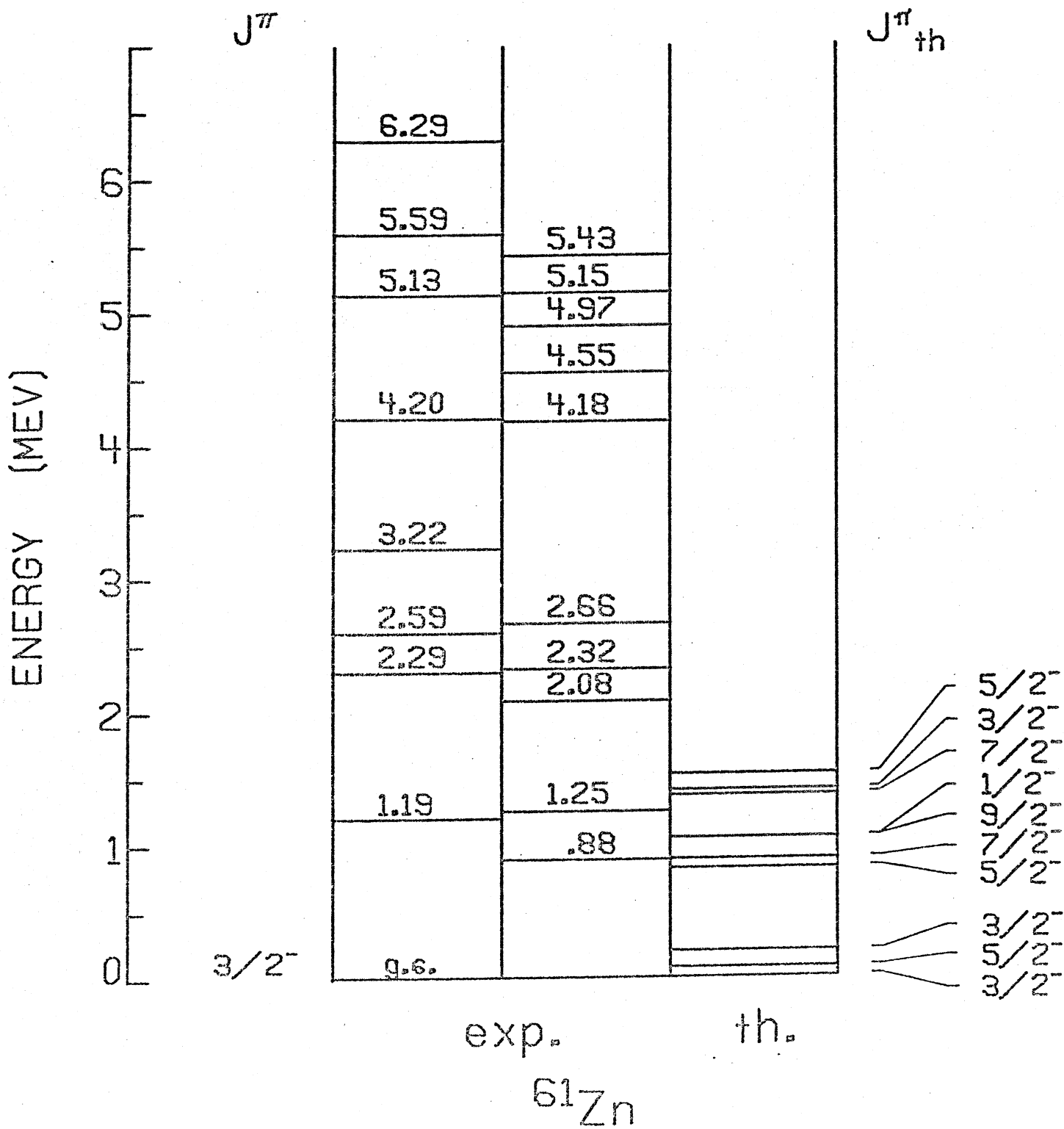
θ_{cm}



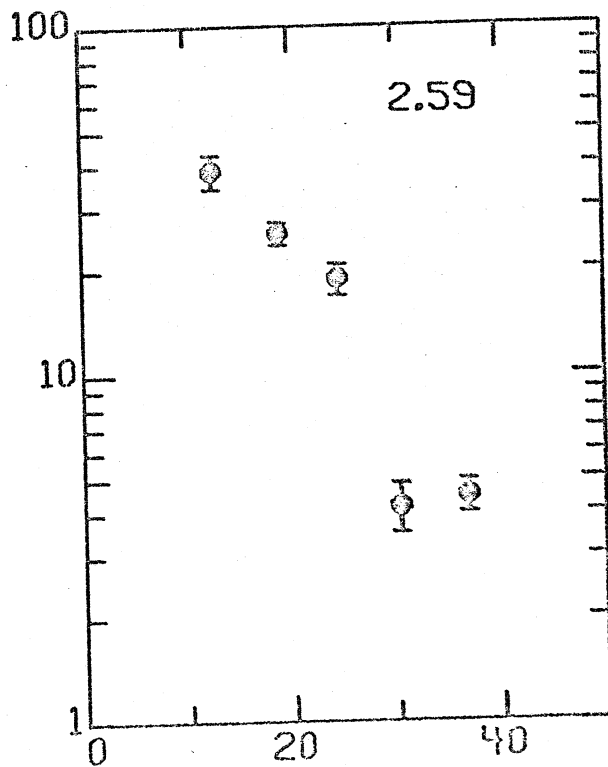
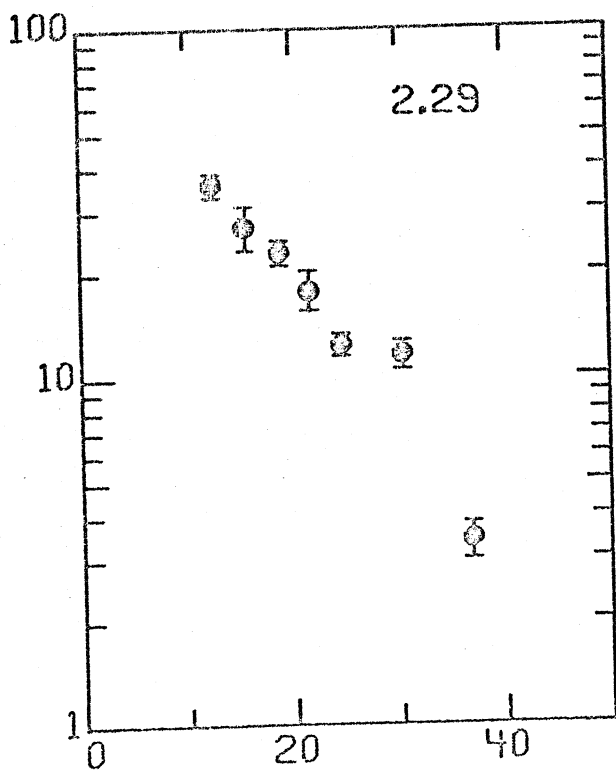
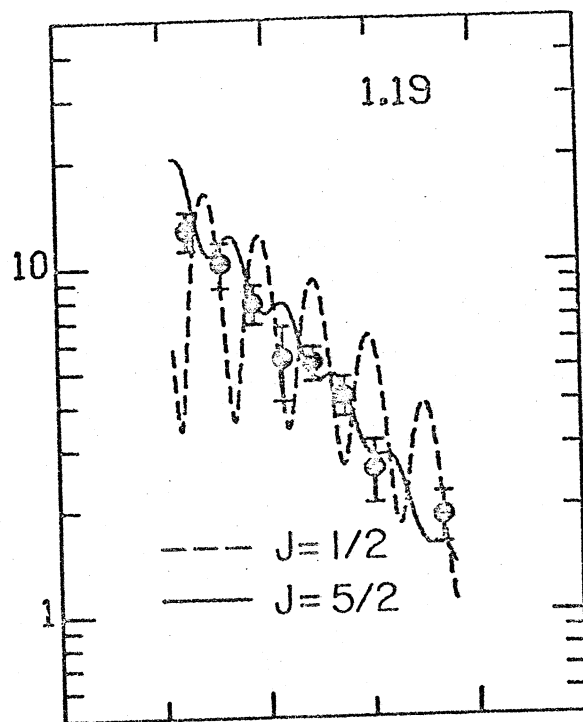
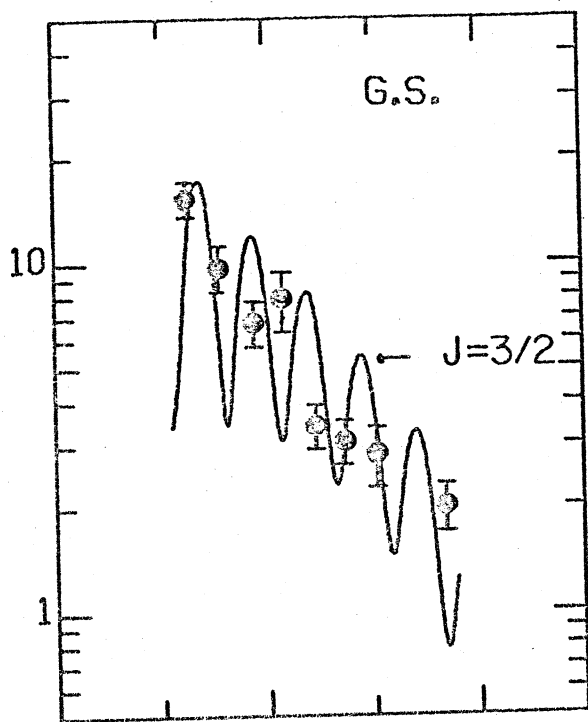
θ cm



$(^{12}\text{C}, ^9\text{Be})$ $(^3\text{He}, ^6\text{He})$



σ_{cm} ($\mu b/sr$)



θ_{cm}

